J. Geotech. Eng., JSCE, No.659/ III-52, 1-16, 2000 September

AN APPROACH TO SEISMIC PERMANENT DISPLACEMENT OF SLOPES

Hamid Reza RAZAGHI[1], Eiji YANAGISAWA[2] and Motoki KAZAMA[3]

[1]Member of JSCE, Ph.D. Student, Civil Eng. Dep., Tohoku University (Aramaki Aoba 06, Aoba-ku, Sendai 980-8579)
[2]Fellow of JSCE, President, Hachinohe National College of Technology (Tamonoki, Uwanotai 16-1, Hachinohe 039-1104)
[3]Member of JSCE, Associate Professor, Civil Eng. Dep., Tohoku University (Aramaki Aoba 06, Aoba-ku, Sendai 980-8579)

A new concept of Newmark's sliding block method for predicting permanent displacements of earth slopes subjected to seismic loading is presented. Horizontal ground acceleration is used as input motion to move a rigid circular sliding block inside an embankment. The effect of the maximum ground horizontal acceleration, velocity and displacement; the maximum value of the response spectrum of the earthquakes for acceleration, velocity and displacement, the values of the response spectrum corresponding to the maximum permanent displacement; and spectrum intensity as well as predominant frequency of the earthquake acceleration on the permanent displacement are studied.

Key Words: *earth slope, seismic loading, permanent displacement, earthquake, rigid circular block*

1. INTRODUCTION

The analysis and design of earth slopes and embankments under seismic loading conditions have been a topic of considerable interest in geotechnical engineering practice for about four decades. During that period, the state of design practice has moved from simple pseudo-static analyses to more complicated permanent displacement analyses. The pseudo-static method is the most common approach for the seismic design of soil structures such as earth dams, embankments and retaining walls. The basic premise in pseudo-static methods is that the soil structure behaves as a rigid plastic material and is at a state of limit equilibrium under the action of acceleration-induced inertial forces super-imposed on static forces. The pseudo-static approach is incapable of quantifying the extent to which the soil structure has been displaced. This inadequacy has long been recognized and many displacement-based methods have been developed as an alternative approach.

A variety of analytical tools ranging from sliding block analyses to multi-dimensional nonlinear dynamic response analyses are now available for prediction of permanent displacements. These tools represent the mechanics of the seismic slope stability problem with different levels of rigor and accuracy, and require different levels of information on material behavior. The most useful are those that can represent the important physical mechanisms of a particular seismic stability problem using material information that can be obtained practically and economically.

The present paper deals with characteristics of seismic forces that might affect the safety of slopes, from the standpoint of seismic slope stability of the conventional circular slip surface method. It presents a new approach to the prediction of permanent slope displacements that accounts for important physical mechanisms of earth slope behavior that are not taken into consideration by most existing methods of analysis.

2.THE ADVANTAGES AND LIMITATIONS OF VARIOUS METHODS OF ANALYSIS

The seismic stability of slopes can now be analyzed by a variety of methods. In the following, the advantages and limitations of the various methods of analysis are reviewed.

Pseudo-static analyses represent the transient effects of an actual earthquake motion by applying constant uni-directional acceleration to a mass of potentially unstable material. The magnitudes of the horizontal and vertical pseudo-static loads are usually expressed in terms of seismic coefficients, k_h and k_v, numerically equal

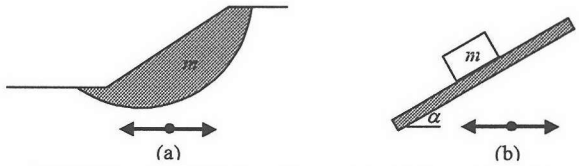

Fig. 1 Schematic illustration of conventional Newmark model

to the ratios of the inertial forces to the weight of the unstable mass. The pseudo-static factor of safety provides an index of stability under seismic conditions. Selection of an appropriate seismic coefficient, however, is a crucial and complicated matter[1),2),3),4)]. However, the pseudo-static factor of safety provides no information on potential slope deformations and does not taken into consideration the dynamic response of soil structures and consequently resonant state that is an important factor in dynamic problems.

The post-earthquake serviceability of a slope can fundamentally be related more to the permanent deformations that develop during shaking than to the factor of safety. Newmark[5)] developed a simple procedure for estimation of permanent slope displacements due to earthquake shaking. By assuming the material above the failure surface to be rigid, he showed that the seismic slope stability problem was analogous to the problem of a rigid block resting on an inclined plane (**Fig. 1**). A block on a plane will move together with the plane as long as the inertial force acting on the block parallel to the plane does not exceed the frictional force that resists relative movement between the block and the plane. When this frictional force is exceeded, the block can no longer accelerate as fast as the plane, and the block moves relative to the plane. The movement continues until the inertial force drops below the frictional force and the velocity of the plane coincides with that of the block. Knowing the yield acceleration and the time history of base acceleration, permanent displacements can be calculated by a straight-forward double integration process.

The materials that comprise most slopes, however, are deformable rather than rigid; this is particularly true for landfills[6)]. As earthquake waves propagate through a slope, different parts of the slope vibrate at different amplitudes and with different phases. The extent to which the compliance deformability of the slope deviates from Newmark's conventional assumption of rigidity depends primarily on the relationship between the wavelength of the motion and the size of the potential failure mass. For deep sliding masses and/or short wavelengths, the effect may be considerable. An approach to the estimation of the resultant driving force developed by Chopra[7)] has been used to estimate pseudo-static coefficients[8)] and permanent embankment displacement[9)]. A one dimensional analog to this procedure[10),11),12),13)], has been applied to landfills. In this procedure the effects of failure mass compliance and the permanent displacements are computed separately, or "decoupled". The decoupled procedure assumes that the dynamic response of the potential failure mass is not influenced by permanent displacement that occurs on the failure surface. The validity of the decoupling assumption has been investigated in the context of earth dam stability by Lin and Whitman[14)]. After subjecting the idealized model to harmonic and simulated earthquake motions, Lin and Whitman concluded that the decoupled approach provided a somewhat conservative estimation of permanent displacement. The conservatism was the greatest at the fundamental period of the dam, but the overall errors were considered to be insignificant relative to other sources of uncertainty inherent in sliding block analyses.

Kramer and Smith[6)] developed a modified version of the Newmark analysis that accounts for the dynamic response of a landfill. In this analysis, the single rigid block of the conventional Newmark analysis is replaced by two or more blocks connected by springs and dashpots. In the two-mass form, the total mass of the material above a potential failure surface is divided into two separate masses (**Fig. 2**). The lower mass rests on an inclined plane with interface friction and the upper mass is connected to the lower mass by a spring and dashpot. The distribution of total mass between the upper and lower masses is described by the mass ratio. The equation of motion is solved for the upper and lower mass simultaneously.

In these methods, there is no way to consider

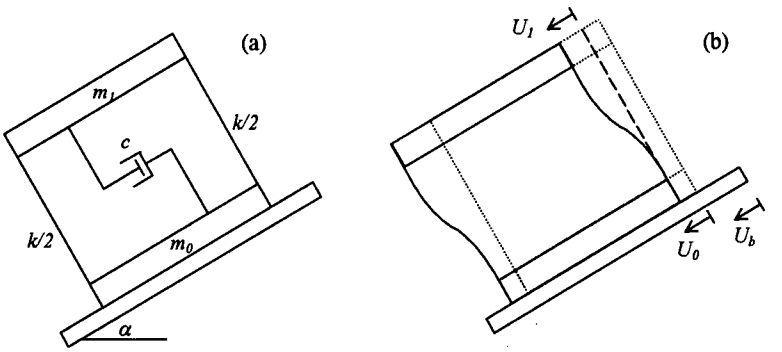

Fig. 2 Modified Newmark model: (a) Schematic illustration; (b) Notation used to describe displacement of modified Newmark model

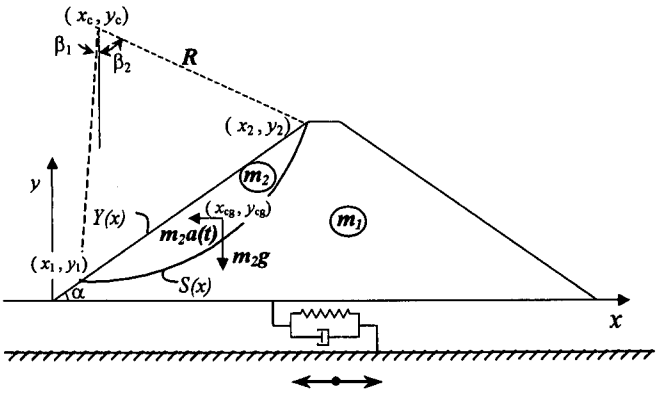

Fig. 3 Notations and schematic illustration of circular sliding block inside an earth slope

the dynamic response of the slope body. The natural frequency of an earth slope and damping of constituent materials that may play a significant role in resonance condition and permanent slope displacement are not taken into account.

3. DEVELOPING OF A NEW MODEL

(1) Critical slip surface and yield acceleration

To develop a method of seismic slope stability analysis that takes into account the dynamic response of an earth slope and the effect of the natural frequency of the slope, a new model of the Newmark analysis is developed. The shape of slip surface for a c-ϕ soil is a curve that is approximated as a circle by many researchers including Bishop[15]. In this new model, it is assumed that the rigid block of the conventional Newmark analysis is a circular one that rotates relative to the failure surface during shaking. The slope is connected to the ground by a spring with a stiffness k and a dashpot with a coefficient of C. It behaves in the manner of a mass spring system with one degree of freedom until the rigid block begins to slide.

Fig. 3 illustrates a soil slope with a slope angle of α which has strength parameters of c and ϕ and which is subjected to horizontal acceleration, $a(t)$. The permanent rotational displacement of the circular rigid sliding block is estimated by simultaneously solving the equation of motion for the earth slope body and the circular rigid block.

To determine the critical slip surface, pseudo-static analysis is used. Assuming that the input acceleration is constant, the safety factor is calculated based on the conventional stability analysis. By solving for the moment equilibrium of the potentially unstable soil, a pseudo-static factor of safety can be computed. The minimum safety factor of the case is determined by changing the radius and the coordinates of the center of the slip circle at a certain acceleration. Because the material above the potential failure surface is assumed to be rigid, the acceleration is taken as a constant inertial force acting on the block. The acceleration at which the inertial force is equal to the resisting force and at which slip begins can be defined as the yield acceleration; it is usually taken as the minimum acceleration that produces a computed factor of

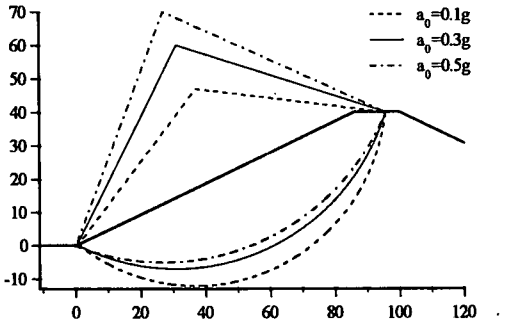

Fig. 4 critical slip surface for various acceleration

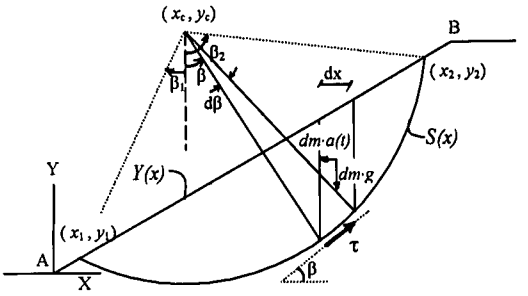

Fig. 5 Notation used to calculate driving moment and resisting moment

safety against rotational displacement equal to unity. The circle corresponding to this case is defined as the critical slip surface. **Fig. 4** shows the critical slip surface for three different values of seismic coefficients: $0.1g$, $0.3g$ and $0.5g$. As can be seen, when the acceleration increases, the circles approach a unique one. For acceleration more than 300 Gal, the critical slip surface can be approximated as a unique one. Therefore, it is assumed that the slip surface is not changed during seismic loading. This assumption is valid for the other combination of α, c, ϕ and γ.

(2) Rotation of a circular rigid sliding block

A sliding block resting on the critical circular slip surface in the slope is assumed to be rigid, and the slope is subjected to a time history of acceleration of $a(t)$. Newmark's method and the equation of motion are used to determine the angular velocity and rotation of the rigid block during a certain period of time. The gravitational force and inertial force cause both the driving moment and the resisting moment. Considering rotational movement of the circular rigid block in **Fig. 3**, the driving moment, M_D, is easily obtained by

$$M_D = mg(x_{cg} - x_c) + ma(t)(y_c - y_{cg}) \qquad (1)$$

where x_{cg} and y_{cg} are the coordinates of the gravitational center of the circular block, and x_c and y_c are the coordinates of the center of the circle. To obtain the resisting moment, consider a potential sliding mass which is bounded by a circular slip surface $S(x)$ and a slope surface $Y(x)$ as illustrated in **Fig. 5**. The resisting moment is divided into two parts. One is the moment corresponding to the cohesion and the frictional force which acts on the sliding surface, M_{R1}, and the other is the moment corresponding to excess frictional force caused by the normal component of inertial force on the sliding surface, M_{R2} . Assuming a small element inside the sliding mass (**Fig. 5**), M_{R1} can be written as

$$M_{R1} = \int_{\beta_1}^{\beta_2} R.\tau.Rd\beta = R^2 \int_{\beta_1}^{\beta_2} \tau.d\beta \qquad (2)$$

where

$$\tau = [Y(x) - S(x)]\,\gamma \cos\beta \tan\phi + c \qquad (3)$$

$$Y(x) = x \tan\alpha \qquad (4)$$

$$S(x) = y_c - \sqrt{R^2 - (x - x_c)^2} \qquad (5)$$

Substituting equations (3), (4), (5) into (2) results in

$$M_{R1} = R^2 \gamma \tan\phi\,(I_1 + I_2) + R^2 I_3 \qquad (6)$$

Where

$$I_1 = \int_{\beta_1}^{\beta_2} x \tan\alpha \cos\beta\, d\beta$$

$$I_2 = \int_{\beta_1}^{\beta_2} \left(-y_c + \sqrt{R^2 - (x - x_c)^2}\right) \cos\beta\, d\beta$$

$$I_3 = \int_{\beta_1}^{\beta_2} c\, d\beta$$

Solving the latter equation, gives M_{R1} as

$$M_{R1} = R^2 c(\beta_2 - \beta_1) + R\gamma \tan\phi \left\{ \begin{array}{l} \dfrac{x_2^2 - x_1^2}{2} \tan\alpha - y_c(x_2 - x_1) \\ +\dfrac{1}{2}\left[\begin{array}{l} (x_2 - x_c)\sqrt{R^2 - (x_2 - x_c)^2} \\ -(x_1 - x_c)\sqrt{R^2 - (x_1 - x_c)^2} \end{array} \right] \\ +\dfrac{1}{2} R^2 (\beta_2 - \beta_1) \end{array} \right\} \qquad (7)$$

The small resisting moment due to the tangential

force of the small element that was caused by the inertial force is defined as

$$dM_{R2} = - dm \cdot a(t) \cdot \sin\beta \cdot \tan\phi \cdot R \qquad (8)$$

where

$$dm = [Y(x) - S(x)]\, dx \cdot \gamma / g \qquad (9)$$

Therefore,

$$M_{R2} = \int_{x_1}^{x_2} -R[y(x) - S(x)]\frac{a(t)}{g}\gamma.\sin\beta.\tan\phi.dx \qquad (10)$$

Substituting equations (4) and (5) into (10) and solving it, results in

$$M_{R2} = -\frac{a(t)}{g}\gamma.\tan\phi\left\{\begin{array}{l}\left(\frac{x_2^3 - x_1^3}{3} - \frac{x_2^2 - x_1^2}{2}x_c\right)\tan\alpha \\ -\frac{x_2^2 - x_1^2}{2}y_c + (x_2 - x_1)x_c y_c \\ -\frac{[R^2 - (x_2 - x_c)^2]^{3/2} - [R^2 - (x_1 - x_c)^2]^{3/2}}{3}\end{array}\right\} \qquad (11)$$

$$M_R = M_{R1} + M_{R2} \qquad (12)$$

where α is the inclination of the soil slope, γ is the unit weight of the soil, R is the radius of the circular block, and β_1 and β_2 are the angles shown in **Fig. 3**. While the inertial force acts in the downward direction of the slope, M_{R2} is negative and the total resisting moment decreases. When the direction of the inertial force changes to the upward, the total resisting moment increases. In this latter situation the resistance is so high that it is not usually overcome by the driving moment and the movement will not occur in this direction.

If the absolute value of the driving moment becomes more than the absolute value of the resisting moment, the circular sliding block will rotate. To calculate the displacement, it is necessary to solve two equations of motion simultaneously. The first one gives the acceleration, velocity and displacement of the earth slope relative to the ground and the second one yields angular acceleration, angular velocity and rotational displacement of the circular sliding block relative to the earth slope. While the resisting moment is larger than the driving moment, the block can not move relative to the slope and consequently the first equation is given by

$$(m_1 + m_2)\ddot{u}_1 + c\dot{u}_1 + ku_1 = (m_1 + m_2)\ddot{u}_0 \qquad (13)$$

where m_2 is the mass of the circular block, m_1 is the mass of the earth slope subtracted from that of the circular block, $\ddot{u}_1, \dot{u}_1, u_1$ are acceleration, velocity and displacement of the earth slope relative to the ground and $\ddot{u}_0$ is the ground acceleration. Direction of the ground acceleration is opposite the direction of the acceleration of the earth slope. Equation (13) can be rewritten as

$$\ddot{u}_1 + 2\xi n_0\dot{u}_1 + n_0^2 u_1 = \ddot{u}_0 \qquad (14)$$

where

$$n_0 = \sqrt{k/(m_1 + m_2)} \qquad (15)$$

and ξ is the damping ratio. On the other hand, it is possible to calculate n_0 from the natural frequency of the slope, f_n:

$$n_0 = 2\pi f_n \qquad (16)$$

When the driving moment becomes more than the resisting moment, the circular block will slide and the first equation of motion is obtained as

$$m_1\ddot{u}_1 + c\dot{u}_1 + ku_1 = m_1\ddot{u}_0 - F_R \qquad (17)$$

where F_R is the horizontal component of resisting force between interface of the block and the slope. Equation (17) is rewritten as

$$\ddot{u}_1 + 2\xi n_1\dot{u}_1 + n_1^2 u_1 = \ddot{u}_0 - F_R/m_1 \qquad (18)$$

where

$$n_1 = \sqrt{k/m_1} \qquad (19)$$

To obtain rotational displacement of the circular block, let's assume the angle of rotation at time t as θ; the center of gravity of the circular block will traverse a curve measured as $R_{cg}\theta$ and each point of the interface between the block and the slope will traverse a curve measured as $R\theta$. $a(t)$ is summation of the acceleration of the slope and the ground acceleration. The second equation of motion for the circular block is given by

$$R_{cg}^2 m_2\ddot{\theta} = M_D - M_R \qquad (20)$$

where R_{cg} is the distance from center of the slip circle to the gravitational center of the block, m_2 is the mass of the sliding block and $\ddot{\theta}$ is the angular acceleration of the rigid block that causes rotation. As initial conditions for solving this equation, angular velocity and rotational displacement at t=0 are given as zero. If the absolute value of the driving moment is less than that of the resisting moment, there is no relative movement:

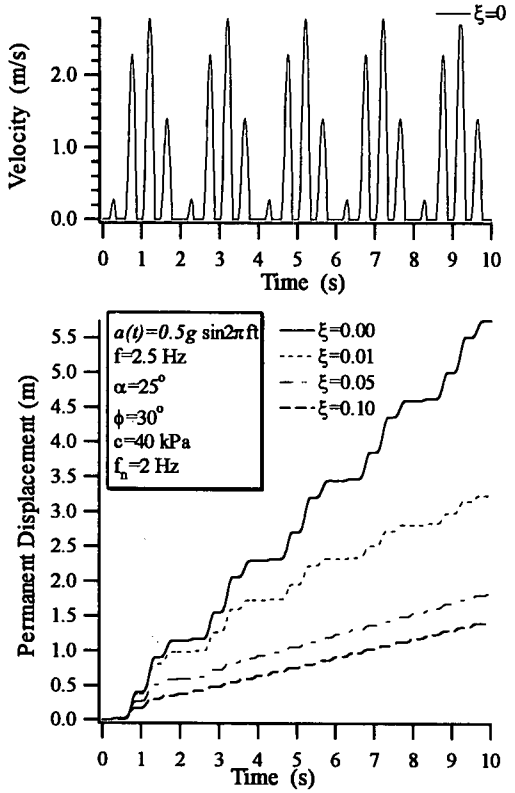

Fig. 6 Angular velocity and displacement during sinusoidal shaking. Effect of damping is shown for displacement.

$$\ddot{\theta} = 0 \quad \text{when} \quad |M_D| \le |M_R| \qquad (21)$$

When $|M_D|$ becomes greater than $|M_R|$, sliding occurs, and rotational displacement starts and continues until the inertial force acting on the failure mass reverses; furthermore, the relative angular velocity between the block and the slope becomes zero.

4. HARMONIC WAVES AS INPUT MOTION

(1) Permanent displacement due to sinusoidal shaking

To analyze the seismic stability of a slope, the permanent displacement is calculated by direct integration of the equation of motion. Both the harmonic wave and random shaking are employed. The harmonic wave is used first because it is possible to change a characteristic of a harmonic motion like the maximum amplitude or the frequency while keeping the other characteristics constant. As a representative model of an earth structure, a slope with values of $\alpha=25^\circ$, $\phi=30^\circ$, c=40 kpa and $\gamma=18$ KN/m^3 is assumed. The height of slope is defined as 50 m. The radius of slip circle and the coordinates of the center of circle are R=66 m, x_c=32 m and y_c=58 m, respectively.

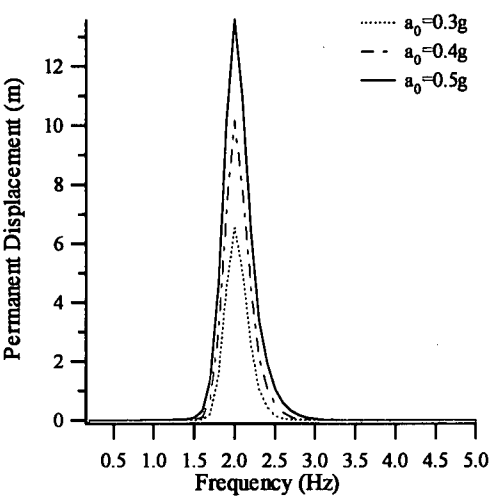

Fig. 7 Effect of frequency on the displacement for different Accelerations (ξ=0.05, t=5 s)

The natural periods of embankment dams have been actually measured by Okamoto[16]. It shows that in the direction perpendicular to dam axis, the natural periods changes from 0.23 to 0.5 second for different dams. In other words the natural frequency of earth slopes is between 2 Hz and 4.3 Hz. The natural frequency of the model of the slope is assumed to be the minimum value, i.e. 2 Hz. The input sinusoidal acceleration wave is defined as $u_0(t)=0.5g\sin 2\pi ft$, where f is the frequency of input motion which is given as 2.5 Hz and the duration of shaking is set to be 10 seconds. The angular velocity, $R\dot{\theta}$, and the rotational displacement, $R\theta$, versus time are calculated. $R\theta$ is the curve that is traversed by circular rigid block during shaking which is positive when it occurs in downward direction. Hereafter $R\theta$ is designated as permanent displacement of circular rigid block.

Equations and graphs for determination of damping of soils involving repeated loading or vibration of soils have been presented by Hardin and Drnevich[17]. These equations and graphs are based on test on saturated cohesive soils and on clean sands. The damping ratio depends on the stress-strain relations for soil and the number of cycles of dynamic loading. Once shear strain increases, the damping ratio increases. The values of damping ratio for cohesive soils is less than 25% and for clean sands is less than 30%, but for the most cases this value is less than 10%. Herein, the values of damping ratio is changed from 0 to 10% to show the

Table 1 The characteristics of earthquake waves used in this study

Earthquake Name	Observed station	Elevation	Direction	Peak Acceleration (Gal)		Max Velocity (cm/s)	Max Dis. (cm)	SI (cm/s)	Duration (s)	Δt (s)
				+	-					
1983 Nihonkai Chubu	Akita Port	Incident wave	E-W	143	-106	21.7	3.6	52.9	20	0.01
			N-S	122	-153	21.9	3.1	57.6		
1994 Hokkaido Nansei-oki	Hakodate Port	ground surface	E-W	104	-115	25	12.7	42.3	240	0.01
			N-S	118	-114	32.3	13.7	50.9		
1995 Hyogo-ken Nambu	JMA Kobe	ground surface	E-W	617	-477	36.7	4.6	49	25	0.01
			N-S	579	-818	45.9	5.2	63.8		
1995 Hyogo-ken Nambu	Kobe Port Island	GL. -83.5m	E-W	335	-688	66.3	25.8	97.3	100	0.01
			N-S	280	-303	29.6	11.1	45.2		
1995 Hyogo-ken Nambu	Kobe Port Island	GL -32.5m	E-W	374	-544	65.1	28.1	120.5	100	0.01
			N-S	462	-258	59	21.9	92.5		
1995 Hyogo-ken Nambu	Kobe Port Island	GL -16.5m	E-W	565	-343	76.8	31.1	144.7	100	0.01
			N-S	543	-209	53.4	25.8	106.2		
1995 Hyogo-ken Nambu	Kobe Port Island	GL. 0.0 m	E-W	284	-183	48	21.1	80.5	40	0.01
			N-S	215	-341	71.7	27.3	129.7		
1993 Kushiro-oki	Kushiro Port	ground surface	E-W	344	-294	27.1	5.3	53.3	100	0.01
			N-S	351	-469	61.3	17	112.3		
1989 Loma prieta	Fire station	ground surface	E-W	628	-510	56.1	5.1	75.7	25	0.005
			N-S	481	-353	40.4	5.4	80.8		
1972 Managua	Comp East	ground surface	E-W	285	-351	29.3	7.5	47.6	46	0.02
			N-S	319	-296	30.5	6.2	53.8		
1994 Hokkaido Nansei-oki	Muroran Port	ground surface	E-W	214	-187	14	6.4	23.2	180	0.01
			N-S	181	-218	13	5.3	20.1		
1994 Sanriku Haruka-oki	Hachinohe Port	ground surface	E-W	493	-676	46.1	13.2	96.7	100	0.01
			N-S	427	-470	34.3	10.4	59.8		

influence of damping on the permanent displacement.

In **Fig. 6**, the velocity against time and the amounts of permanent displacement for different values of the coefficient of damping due to the harmonic excitation are plotted. This figure shows stepwise displacement of the block whose movement ceases when the acceleration reverses, and the velocity in the upward direction becomes zero. As time passes the displacement increases. As shown in this figure, by considering a damping ratio of only 1%, the displacement after 10 seconds is reduced from 5.76 m without damping to 3.24 m for a damping ratio of 1%. If the damping coefficient increases, the displacement becomes smaller. For 10% damping, the total displacement is reduced to 1.46 m.

(2) Effect of frequency of input waves

Considering the mass and spring system for connecting the earth slope to the ground, the effect of the natural frequency of the embankment and the frequency of the input waves are taken into consideration. To show the effect of the frequency of seismic excitation, it is again assumed that the natural frequency f_n is 2 Hz and that the time history of dynamic loading is 5 seconds. **Fig. 7** shows a plot of displacement of circular block after 5 seconds versus different frequencies of input waves. It can be seen that the displacement will increase when the input frequency is close to the natural frequency. Maximum displacement corresponds to $f = f_n$ (i.e. resonance condition). Even if the input acceleration is less than the yield acceleration of the critical circular slip surface which is defined in the previous section, there might be a kind of amplification by the system. Furthermore, the slope will sometimes fail and considerable rotation of the sliding mass in the slope will take place under the resonance condition and also in a range of frequencies around the natural frequency. In other words, the ratio of the frequency of input waves to the natural frequency of the slope has a considerable influence on the displacement. This means pseudo-static solutions do not always gives conservative results, at least when the frequency of input waves is sufficiently close to the natural frequency.

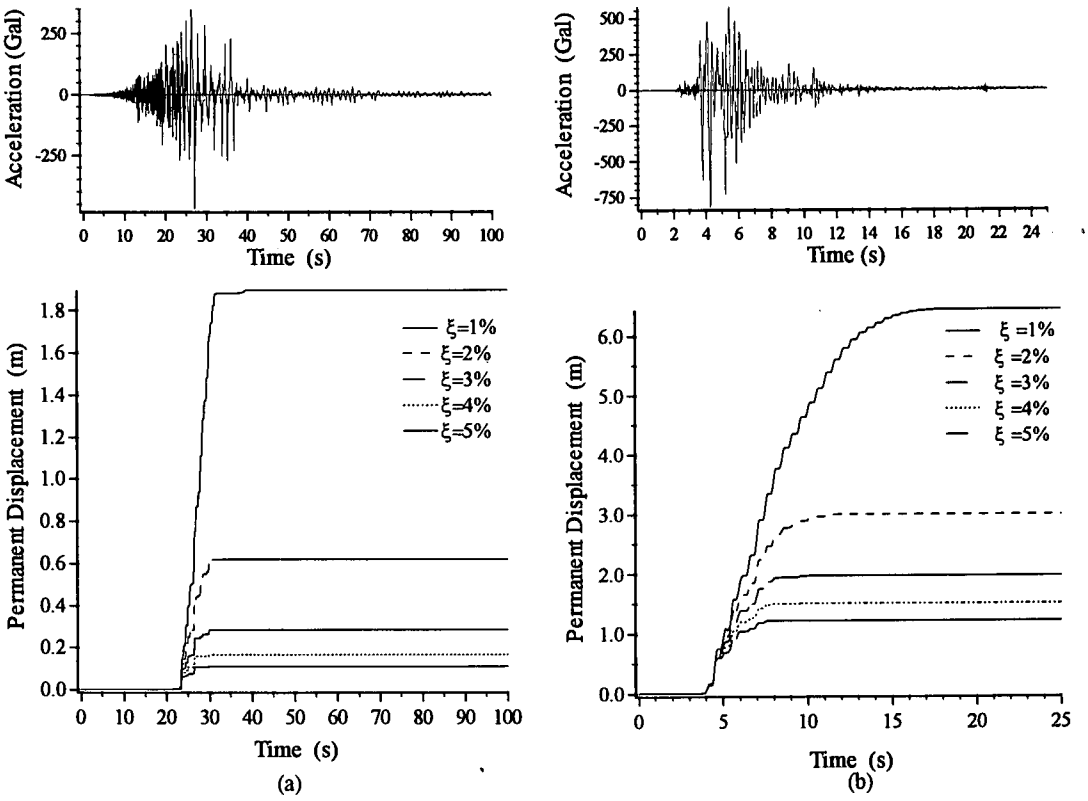

Fig. 8 Acceleration records, and permanent displacement versus time during earthquake for various coefficients of damping, (a) Kushiro earthquake, (b) Kobe earthquake

5. PERMANENT DISPLACEMENT DUE TO RANDOM SHAKING

(1) Permanent displacement during seismic excitation

For engineering purposes, the responses of slopes to real earthquakes must be studied. For this purpose, random shaking based on twenty-four records of acceleration due to eight earthquakes are employed as input waves to analyze the permanent displacement of a slope. The characteristics of the earthquakes are listed in the **Table 1**. As an example, the same slope model is used with a slope angle of $\alpha=25^{\circ}$, whose strength parameters are $\phi=30^{\circ}$ and $c=40$ kpa. The natural frequency of the slope is assumed to be 2 Hz. Direct integration is used to solve the equation of motions for calculating the permanent displacement.

To show sample results of the permanent displacement in the time domain during earthquake motion, two earthquake records of acceleration are used. One is the N-S component of the Kobe earthquake, the strongest motion with the largest maximum amplitude among 24 waves. The other is the N-S component of the Kushiro earthquake for which calculation of the maximum permanent displacement showed that in a specific case, this earthquake yields the largest maximum permanent displacement. This matter will be explained in detail in the next section.

Figs. 8(a) and **8(b)** show the recorded waves of the Kushiro and Kobe earthquakes as input motion and calculation of the displacements of the circular sliding block in time domain, respectively. It is assumed that the damping coefficient changes from 1% to 5%. As shown in this figure, the displacement diagram is again stepwise. The total displacement of the circular block after ceasation of the earthquake is defined as permanent displacement.

It can be seen that the permanent displacement for this case due to the Kushiro earthquake changes from 1.9 m for 1% damping to 11 cm for 5% damping. For the case of the Kobe earthquake, it changes from 6.43 m for 1% damping to 1.23 m for 5% damping ratio. As expected, herein, the permanent displacement of the Kobe earthquake is considerably more than that of the Kushiro earthquake (about eleven times for 5% damping).

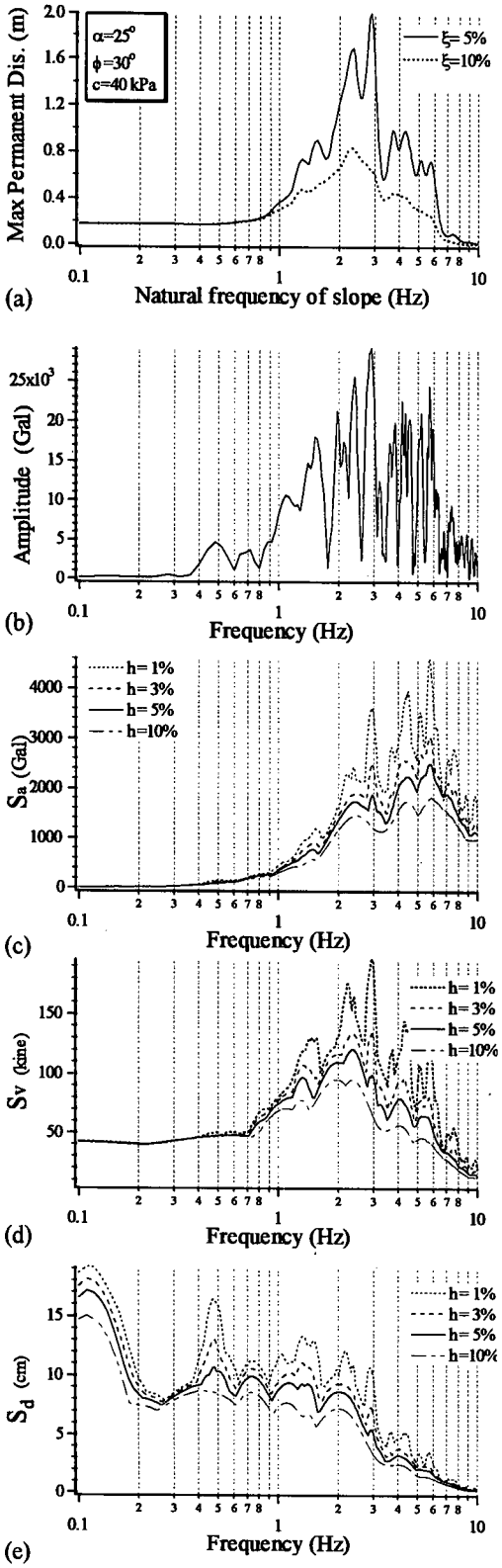

Fig. 9 Analysis of Kobe earthquake wave (a) maximum permanent displacement versus natural frequency of slope, (b) Fourier Spectrum, (c) acceleration response spectrum, (d) velocity response spectrum, (e) displacement response spectrum.

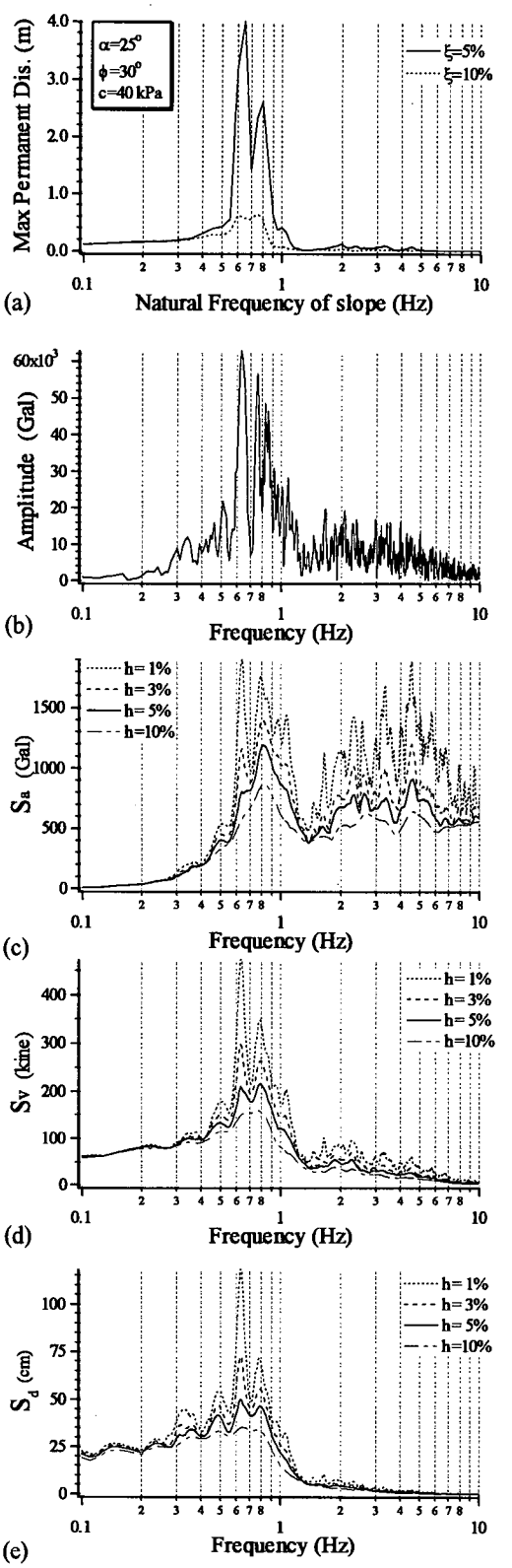

Fig. 10 Analysis of Kushiro earthquake wave (a) maximum permanent displacement versus natural frequency of slope, (b) Fourier Spectrum, (c) acceleration response spectrum, (d) velocity response spectrum, (e) displacement response spectrum.

(2) Influence of earthquake waves

To evaluate the influence of the natural frequency of the slope on the permanent displacement, the permanent displacement at the end of the earthquake is calculated for slopes with different natural frequencies. Then, the maximum is obtained by changing the natural frequency of the slope. The Kobe and Kushiro earthquakes are again employed to show the different characteristics of waves in more detail.

As shown in the previous section, in harmonic motion the ratio of the frequency of input waves to the natural frequency of the slope has a considerable influence on the permanent displacement. It is expected that the ratio of the predominant frequency of earthquake acceleration to the natural frequency of the slope affects the permanent displacement. To observe this effect, the natural frequency of the slope is changed from 0 to 10 Hz. Then the permanent displacement of each case is calculated for the two earthquake records. **Figs. 9(a)** and **10(a)** show the permanent displacement against the natural frequency for two cases of damping, i.e., 5% and 10% due to the Kobe and Kushiro earthquakes, respectively. It can be seen that the maximum displacements for the Kobe and Kushiro earthquakes occur when the natural frequency becomes 2.9 Hz and 0.65 Hz, respectively.

The Fourier spectrum is obtained to determine the predominant frequency of the earthquake waves. The results are shown in **Fig. 9(b)** and **10(b)** for the Kobe and Kushiro earthquakes, respectively. It can be seen that the predominant frequency of the Kobe earthquake is 2.9 Hz and that of the Kushiro earthquake is 0.65 Hz. These two frequencies are exactly the same as the frequencies of the maximum permanent displacements for the Kobe and Kushiro earthquakes (**Figs. 9(a)** and **10(a)**); there is good agreement between the predominant frequency and the frequency for maximum permanent displacement in both cases.

It is worthwhile to evaluate the relation among the response spectra, the maximum permanent displacement and the natural frequency of slope. For these purposes, the response spectra for acceleration, velocity and displacement corresponding to the two earthquakes acceleration records are obtained. **Figs. 9(c)** to **9(e)** and **Figs. 10(c)** to **10(e)** show the results of the Kobe and Kushiro earthquakes, respectively.

By comparing **Fig. 10(a)** with **Fig. 10(c)**, it can be seen that the maximum displacement occurs at the same frequency as that of the maximum S_a. But this is not true for the Kobe earthquake (**Figs. 9(a)** and **9(c)**). However, in many cases not shown here,

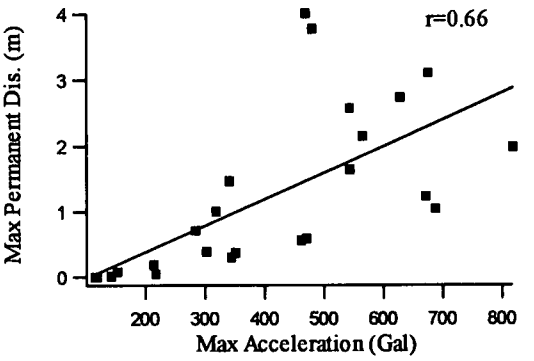

Fig. 11 Maximum permanent displacement of slope versus maximum amplitude of earthquake wave

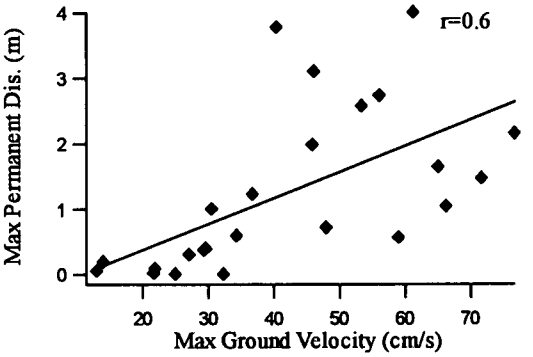

Fig. 12 Maximum permanent displacement of slope versus maximum velocity of ground

there is a good correlation between the natural frequency of the slope for the maximum displacement and one of the peaks of the maximum S_a. In other words, the maximum displacement will occur if one of the peaks of the maximum S_a coincides with the natural frequency of the slope.

As seen in **Fig. 9(d)**, for the natural frequency of the maximum displacement, the same can be said with regard to the peaks of the maximum S_v. From standpoint of the value of the maximum S_v, although the maximum acceleration of the Kushiro earthquake is less than that of the Kobe earthquake, the maximum S_v of the Kushiro earthquake is more than that of the Kobe earthquake (similar to the maximum displacement).

The frequency which gives the maximum S_d for the Kushiro earthquake seems to coincide with the natural frequency of the maximum displacement (**Fig 10(e)**). This is true neither for the Kobe earthquake (**Fig. 9(e)**) nor for most of the other earthquake waves. It can be said that a poor correlation exists between the maximum S_d and the maximum slope displacement.

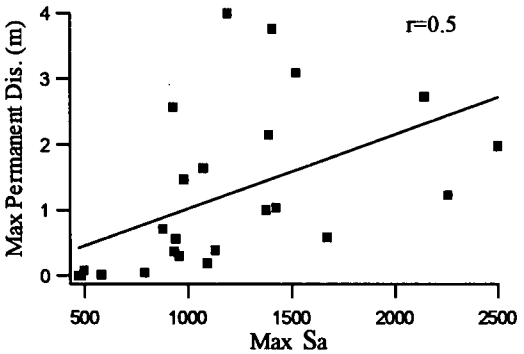

Fig. 13 Maximum permanent displacement of slope versus maximum acceleration response spectra

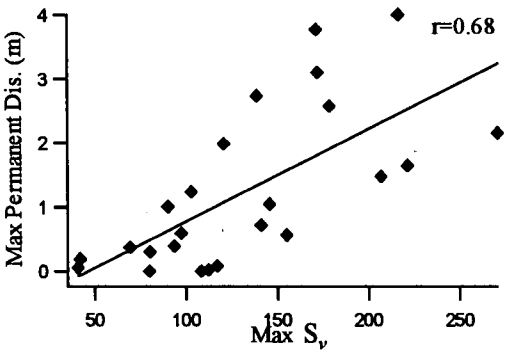

Fig. 14 Maximum permanent displacement of slope versus maximum velocity response spectra

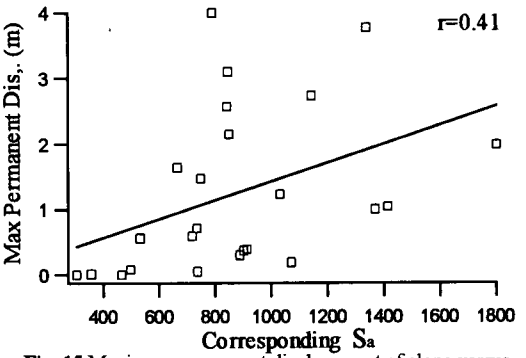

Fig. 15 Maximum permanent displacement of slope versus corresponding S_a

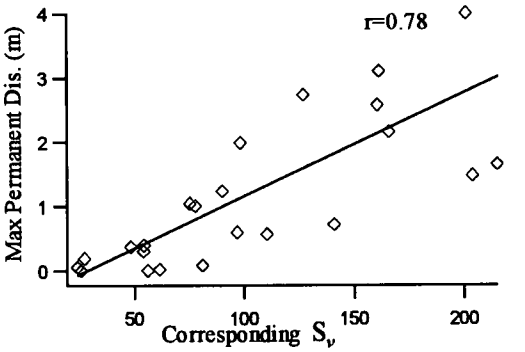

Fig. 16 Maximum permanent displacement of slope versus corresponding S_v

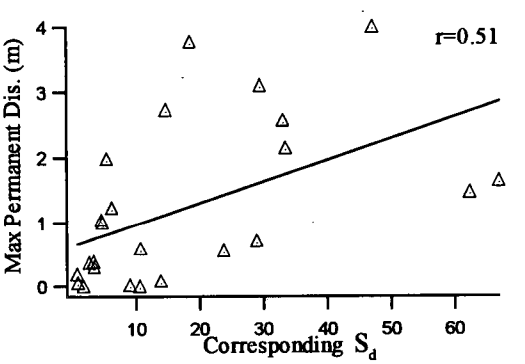

Fig. 17 Maximum permanent displacement of slope versus corresponding S_d

6. EARTHQUAKE CHARACTERISTICS WHICH AFFECT THE MAXIMUM DISPLACEMENT

(1) Seismic waves and characteristics used in the study

To study more about the effect of earthquakes on maximum slope deformations of the circular rigid sliding block, twenty-four acceleration wave records corresponding to the eight strong ground motions including two previously explained earthquakes are employed: Akita, Hakodate, Kobe, Kushiro, Managua, Muroran, Sanriku and Loma Prieta earthquakes, six of which took place in Japan. Waves records correspond to the E-W and N-S components of various stations. These waves are used as input data for the earth slope assumed in the previous section. The results are obtained in the same manner as that employed for the Kobe and Kushiro earthquakes (**Figs. 9** and **10**). The maximum slope displacement and the maximum ground velocity and displacement are also obtained from corresponding diagrams. The maximum response spectra for acceleration, velocity and displacement are obtained from the S_a, S_v and S_d curves against the natural frequency.

One of the parameters that shows the power of earthquake waves is spectrum intensity. To evaluate the effect of this parameter on the maximum displacement, the average of the response spectrum in a range of periods is often used as an index of the intensity of an earthquake. The equation of spectrum intensity is given by

$$SI = \frac{1}{2.4}\int_{0.1}^{2.5} S_v dT \qquad (22)$$

where S_v is the velocity response spectra against period and T is the natural period of system changes

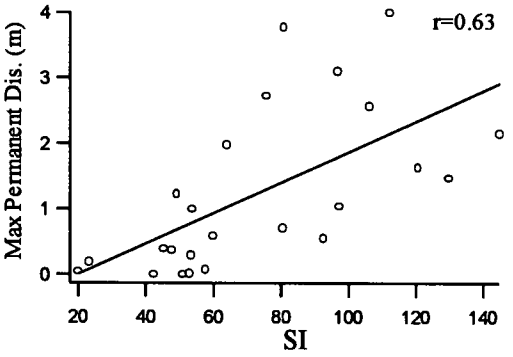

Fig. 18 Maximum permanent displacement of slope versus spectrum intensity

from 0.1 to 2.5 seconds.

To see the effect of the maximum input acceleration, the maximum permanent displacement of 24 waves are plotted against the maximum values of the ground acceleration (**Fig. 11**). Similarly, the maximum permanent displacement versus the maximum ground velocity is plotted as shown in **Fig. 12**. It can be seen that there is a relatively good correlation between the maximum permanent displacement and maximum ground acceleration and velocity. Their correlation factors are 0.66 and 0.6, respectively. To evaluate some other relations, **Figs. 13** and **14** show the effects of the maximum response spectra of input acceleration and velocity for 5% damping on the maximum permanent displacement. As can be seen from a comparison of these two figures, the correlation factors are 0.5, 0.68, respectively, with relatively good correlation in the case of maximum S_v (**Fig. 14**).

To evaluate the seismic effects in more detail, the values of corresponding S_a , S_v and S_d are obtained. The corresponding S_a , S_v and S_d are the values of S_a, S_v and S_d, which are found at the same frequency at which the maximum permanent slope displacement occurs. The damping ratio is assumed to be 5%. **Figs. 15** to **17** show the maximum permanent displacement of slope against corresponding S_a , S_v and S_d. The value of the maximum permanent displacement is also related to the spectrum intensity **SI** as shown in **Fig. 18**. **Figs. 15** to **18** indicate the correlation factors 0.41, 0.78 and 0.51 for the corresponding S_a , S_v and S_d, respectively. Although a clear correlation is not found between the maximum permanent displacement and maximum S_a, corresponding S_a or corresponding S_d, it seems to exist some correlation between the maximum permanent displacement and the maximum acceleration, maximum ground velocity, maximum S_v and corresponding S_v. The best correlation among them is due to the corresponding S_v (**Fig. 16**). **Fig. 18** also shows a

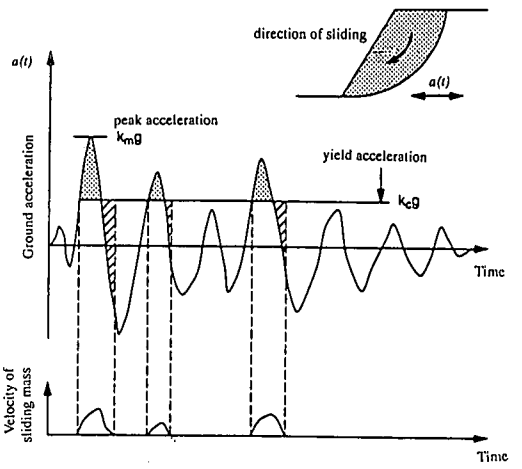

Fig. 19 Illustration of Newmark's sliding block method to calculate permanent displacement of earth slopes

relatively good correlation between spectrum intensity **SI** and the maximum permanent displacement with a correlation factor of 0.63. Among these correlations, it can be clearly seen that the maximum permanent displacement has the best correlation with the corresponding S_v and the maximum S_v, which designate the power of the input earthquake.

(2) Considerations on the specific parameters of earthquake records

With regard to the responses to random shaking, contrary to the case of harmonic excitation, it is quite difficult to change any one of the characteristics of an earthquake acceleration record, such as the predominant frequency of the waves and the frequency component. Furthermore, it can be expected that various characteristics of a wave influence the maximum permanent displacement simultaneously. In **Figs. 11** to **18**, although the maximum permanent displacement has been related to one parameter, in fact, other characteristics of the input waves may also be variables, which affect the maximum displacement. Although we can not see all the marked points in a straight line, the maximum amplitude of input acceleration, the predominant frequency of earthquake waves, the duration of input acceleration and the number of pulses of the wave that are greater than a certain value are significant parameters that affect the maximum displacement. Nevertheless, by comparing the figures, it can be said that the best correlations are obtained for the corresponding S_v , the maximum velocity response spectra and the spectrum intensity **SI** against the maximum permanent displacement.

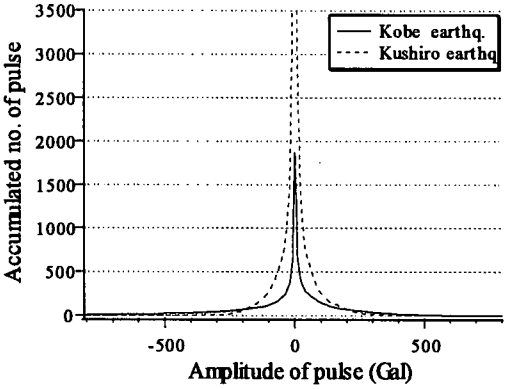

Fig. 20 Number of pulses of different magnitude of amplitude due to Kobe and Kushiro earthquakes acceleration wave

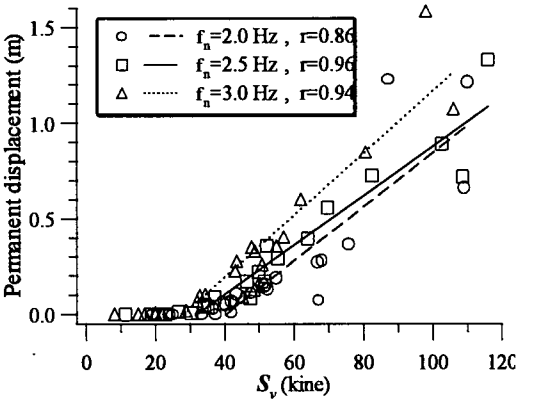

Fig. 21 permanent displacement versus velocity response spectrum in constant frequency

Based on Newmark's method, for a given ground acceleration time history and a known yield acceleration of the sliding mass, earthquake-induced displacement is calculated by integrating those portions of the acceleration history that are above the yield acceleration and those portions that are below until the relative velocity between the sliding mass and the ground is reduced to zero (**Fig. 19**). This integration procedure implies that the momentum is proportional to the hatched area, which is shown in **Fig. 19**.

$$p = mv = F\,\Delta t \tag{23}$$

where p =momentum, m=mass, v=velocity and F=the force acting on the mass during the time of Δt. As the mass is constant, it can be written

$$F\,\Delta t \propto a\,\Delta t \tag{24}$$

where a is acceleration. On the other hand, based on definition, the velocity response spectrum has the same dimension as velocity and is proportional to momentum. As a result;

$$S_v \propto a\,\Delta t \tag{25}$$

It could be concluded that the maximum slope displacement is related to the velocity response spectrum.

(3) The effect of the number of pulses of large amplitude

Let's again compare the Kobe and Kushiro earthquakes. Although the maximum amplitude of the Kobe earthquake acceleration is 818 Gal and is greater than 469 Gal of the Kushiro earthquake, the maximum displacement that is calculated for the earth slope (spesified at section 5.1) subjected to the input wave of the Kobe earthquake is only 1.98 m, less than the maximum displacement of the same slope subjected to the Kushiro earthquake wave, i.e. 4 (see **Figs. 9(a)** and **10(a)**). But we know that contrary to the Kushiro earthquake, the Kobe earthquake destroyed many different kinds of structures, because the power of the Kobe earthquake was more than that of the Kushiro earthquake. By considering **Fig. 9(a)**, it is found that there are two main peaks of maximum permanent displacement for 5% damping corresponding to the Kobe earthquake. The first peak of maximum permanent displacement is 1.98 m that occurred at 2.9 Hz, and the second one is 1.69 m at 2.35 Hz. For 10% of damping, the first peak disappeared and the second one is 0.82 m at 2.35 Hz. Considering **Fig. 9(d)**, it can be seen that the velocity response spectrum for 3% damping corresponding to the Kobe earthquake has two main peaks at 2.9 Hz and 2.35 Hz, and for 5% damping, one peak remains with a value of 120.9 kine at 2.35 Hz. **Fig. 10(a)** shows that at this natural frequency of slope (2.35 Hz) for 5% damping, the permanent displacement caused by the Kushiro earthquake is near zero (0.08 m). This is true for natural frequencies more than 1.1 Hz. **Fig. 10(d)** shows the same thing for the velocity response spectrum corresponding to the Kushiro earthquake, i.e., S_v for 5% damping quickly falls from 217 kine after 0.8 Hz. It is clear that the soil structures have natural frequencies more than 2 Hz and that earthquakes such as the Kobe earthquake can damage and destroy them, but the earthquakes such as the Kushiro earthquake can not seriously damage them. The earth slopes usually have natural frequencies more than 2 Hz and therefore the frequencies less than 2 Hz seems to be unrealistic in the existing dams.

Without considering the differences between the natural frequencies of the maximum permanent displacement for these two earthquakes, it appears

that not only the magnitude of one pulse but also the number of pulses greater than yield acceleration affect the maximum displacement. To evaluate this matter, the number of pulses of different magnitude of acceleration wave is counted at 10 Gal intervals. The distribution of the accumulated number of pulses against the magnitude of the amplitude is illustrated in **Fig. 20** for the Kobe and Kushiro earthquakes. Each point of the respective curves for these two earthquakes shows how many pulses were greater than a certain value of amplitude. As seen in this figure, for example, the number of pulses larger than 180 Gal for the Kobe and Kushiro earthquakes is 79 and 95, respectively, and as second example the number of pulses larger than 120 Gal are 126 and 187, respectively. This may explain the reason for the differences of the value of the maximum displacements between these two earthquakes.

(4) Correlation between the permanent displacement and S_v in constant frequency

As it was seen, the best correlation was between the maximum permanent displacement and the corresponding S_v. It is noteworthy to evaluate this relation in the range of the natural frequencies of real earth structures, which is usually considered to be more than 2 Hz. For this purpose, it is assumed that the natural frequency of the slope is 2 Hz and damping ratio is 5%. Then the permanent displacement of slope and the velocity response spectrum of this frequency for each earthquake are calculated. The correlation between the permanent displacement and S_v is plotted in **Fig. 21**. The correlation for a slope with natural frequencies of 2.5 and 3 Hz is also shown in this figure. As is seen in this figure, there is very good correlation between permanent displacement and S_v with correlations factor of 0.86, 0.96 and 0.94 in the range of the natural frequencies of slopes for 2, 2.5 and 3 Hz, respectively. When S_v is less than a certain value, (for example about 30 kine for f_n=2.5) there is no displacement inside the slope. By increasing S_v the permanent displacement will increase, and the magnitude of it can be related to S_v.

It can be said that there exists a threshold value of velocity response spectrum, from which the permanent displacement of the slope will take place. This fact gives an important information to predict the degree of damage to earth structures for a strong earthquake expected.

7. CONCLUSION

In this paper a new approach to seismic stability analysis of slopes that accounts for important aspects of the seismic stability problem was introduced to clarify the most significant parameters which affect slope stability that have not been accounted for in the most commonly used analyses. Based on the results of this study, the following conclusions can be made.

1) A new aspect of the seismic slope stability is introduced by considering the slope as a vibratory system.
2) When the predominant frequency of an earthquake wave becomes near the natural frequency of the earth slope or at the resonant state, the maximum permanent displacement will considerably increase. This is usually ignored in pseudo-static analysis and determination of the dynamic safety factor. Ignoring this fact may sometimes result in unrealistic findings.
3) There are important input wave characteristics that simultaneously affect the failure of slopes and the magnitude of permanent displacement. These are the time history of earthquake acceleration, the maximum acceleration, the number of pulses larger than the amplitude that causes commencement of failure, the predominant frequency of input acceleration and the natural frequency of the earth slope.
4) Permanent displacement is sensitive to the coefficient of damping. Only by slightly increasing it, the displacement will considerably decrease.
5) The maximum acceleration of input waves affects the increase of the permanent displacement. Increasing the number of pulses of large amplitudes, however, is more effective than maximum amplitude.
6) There is a good correlation between the natural frequency of the maximum permanent displacement and one of the peaks of the maximum S_a. In other words, the maximum permanent displacement will occur if one of the peaks of the maximum S_a coincides with the natural frequency of the slope.
7) The maximum permanent displacement has a relatively good correlation with the maximum ground acceleration and velocity, better than that of the maximum ground displacement.
8) Among the parameters, the best correlation is seen between the maximum permanent displacement and the corresponding S_v, the maximum S_v and the spectrum intensity, **SI**,

which designates the power of the input earthquake.

9) In the range of the natural frequency of actual slopes, the magnitude of the permanent displacement of slopes can be related to the corresponding velocity response spectrum of earthquake waves.

List of Notations

c = cohesion of soil
f = frequency of input
f_n = natural frequency of slope
F_R = horizontal component of resisting force between interface of the block and slope
g = gravity acceleration
m_1 = mass of the earth slope subtracted from that of the circular block
m_2 = mass of the circular block
M_D = driving moment
M_{R1} = resisting moment due to the cohesion and the frictional force
M_{R2} = resisting moment due to excess frictional force caused by the inertial force
M_R = total resisting moment
p = momentum
R = radius of circular slip surface
$S(x)$ = function of circular slip surface
S_a = acceleration response spectra
S_v = velocity response spectra
S_d = displacement response spectra
SI = spectrum intensity
$\ddot{u}_0$ = ground acceleration
$\ddot{u}_1, \dot{u}_1, u_1$ = acceleration, velocity and displacement of the earth slope relative to the ground
x_c, y_c = coordinates of the center of the circle
x_{cg}, y_{cg} = coordinates of the gravitational center of the circular block
$Y(x)$ = function of slope surface
α = slope angle
ϕ = internal friction of soil
γ = unit weight of soil
τ = shear stress
ξ = damping ratio
$\theta(t)$ = angle of rotation of the circular block
$\dot{\theta}$ = angular velocity of the circular block
$\ddot{\theta}$ = angular acceleration of the circular block

REFERENCES

1) Terzaghi, K.: Mechanisms of landslides, *Engineering geology (Berkey) volume*, Geological Society of America, Boulder, Colo., pp.83-123, 1950.
2) Seed, H. B.: Considerations in the earthquake-resistant design of earth and rockfill dams, *Geotechnique*, London, England, 29(3), pp.215-263, 1979.
3) Marcuson, W. F. III.: Moderator's report for session on earth dams and stability of slopes under dynamic loads, *Proc., Int. Conf. on recent adv. In Geotech. Earthquake Engrg. And Soil Dyn.*, Univ. of Missori, St. Louis, Mo., Vol. 3, 1981.
4) Hynes-Griffin, M. E. and Franklin, A. G.: Rationalizing the seismic coefficient method, *Miscellaneous paper GL-84-13*, U.S. Army Corps of Engineers, Vicksburg, Miss, 1984.
5) Newmark, N.: Effects of earthquakes on dams and embankments, *Geotechnique*, London, England, 15(2), pp.139-160, 1965.
6) Kramer, S. L. and Smith, M. W.: Modified Newmark model for seismic displacements of compliant slopes, *J. Geotech Engrg.*,. ASCE, 123(7),. pp.635-644, 1997.
7) Chopra, A. K.: Earthquake effects on dams, PhD dissertation, Univ. of California, Berkeley, Calif, 1966.
8) Seed, H. B. and Martin, G. R.: The seismic coefficient in earth dam design, *J. Soil Mech. And Found. Div.*, ASCE, 92(3), pp.25-58,1966.
9) Makdisi, F. I. and Seed, H. B.: Simplified procedure for estimating dam and embankment earthquake-induced deformations,*J. Geotech. Engrg. Div.*, ASCE, 104(7),. pp.849-867, 1978.
10) Repetto, P. C., Bray, J. D. Byrne,R. J., and Augello, A. J.: Seismic analysis of landfills, *Progress in geotechnical engineering practice*,ASCE Central Pennsylvania Section, Hershey, Pa, 1993.
11) Bray, J. D. and Repetto, P. C.: Seismic design considerations for lined solid waste landfills, *Geotextiles and Geomembranes*, 13, pp.497-518, 1994.
12) Augello, A. J., Bray, J. D., Leonards, G. A., Repetto, P. C. and Byrne, R. J.: Response of lanfills to seismic loading, *Proc. Geoenvironment 2000*, ASCE, New York, N. Y., Vol. 2, pp.1051-1056, 1995.
13) Bray, J. D., Augello, A. J., Leonards, G. A., Repetto, P.C. and Byrne, R. J.: Seismic stability procedures for solid-waste landfills, *J. Geotech. Engrg.*, ASCE, 121(2), pp.139-151, 1995
14) Lin, J. S. and Whitman, R. V.: Decoupling approximation to the evaluation of earthquake-induced plastic slip in earth dams, *Earthquake Engrg. And Struct. Dyn.*, 11(5), pp.667-678, 1983.
15) Bishop, A. W.: The use of the slip circle in the stability analysis of slops, *Geotechnique*, 5, pp.7-17, 1955.
16) Okamoto, S.: Introduction to earthquake engineering, University of Tokyo press, pp.427-490, 1973.
17) Hardin, B. O. and Drnevich, V. P.: Shear modulus and damping in soils: design equations and curves, proc. ASCE, 98(SM7), pp. 667-692, 1972.

(Received September 7, 1999)

斜面の地震時永久変位推定の一手法

Hamid Reza RAZAGHI・柳澤 栄司・風間 基樹

地震荷重を受ける土の斜面の地震時永久変位を予測するために，新たにニューマーク法によるすべりブロックの永久変位の計算方法を提案した．地盤の水平動を入力地震動とし，振動系をなす堤体を剛な円形すべりブロックと残りの本体とに別け，円形ブロックの動きを計算した，永久変形量に及ぼす入力地盤の水平最大加速度，最大速度，最大変位の影響，および加速度，速度，変位の各応答スペクトルとの関係について検討した．